Stochastic model of noise for a quantum thermal transistor

Uthpala N. Ekanayake [1,*] Sarath D. Gunapala,[2] and Malin Premaratne [1,†]

[1]*Advanced Computing and Simulation Laboratory (AχL), Department of Electrical and Computer Systems Engineering, Monash University, Clayton, Victoria 3800, Australia*

[2]*Jet Propulsion Laboratory, California Institute of Technology, Pasadena, California 91109, USA*

(Received 8 September 2023; revised 22 November 2023; accepted 28 November 2023; published 14 December 2023)

Our focus in this investigation lies in developing a noise model for a quantum thermal transistor model inspired by its electronic counterpart, with the primary aim of establishing a platform for constructing analogous models. Previous studies on coupled two-level systems-based thermal transistors were focused on their average energy exchange. In this paper, we shift our attention to exploring the stochastic behavior of such thermal transistors due to the disturbances caused to their environment, such as continuous measurements. In the literature, the master equation for the transistor model is derived using the reduced dynamics method. This way, it masks the study of the stochastic nature of the energy flows in the system due to disturbances to the environment. In this paper, we describe a quantum trajectory under measurement theory whose ensemble average unravels the master equation for a quantum thermal transistor. This allows us to analyze the fluctuations and noise levels in the transistor model with greater detail. Then, we produce a numerical solution for the transistor dynamics based on Euler-Maruyama approximation. This helps to establish a model for the thermal transistor, drawing parallels to the small-signal/noise model in an electronic transistor. We define two parameters, thermal conductance and output thermal resistance, to describe the small signal-like model for the thermal transistor. Through these investigations, we seek to gain insights that can help design advanced heat management devices at the quantum level.

DOI: 10.1103/PhysRevB.108.235421

I. INTRODUCTION

Recently, there has been a growing interest in developing a quantum thermal transistor that can effectively regulate heat flow in electronic circuits. The ability to manipulate quantum resources to build such devices will be fruitful in revolutionizing how we manage thermal energy. Extensive research carried out by various research groups proposes several transistor architectures [1–9], also extending to the transistor networks [10]. The latest studies explore the utilization of environmental effects to improve the amplification of these transistors [8,11] and implement quantum logic gates [12]. Despite the progress made, the practical realization of a quantum thermal transistor requires further investigation and refinement. With the primary focus of establishing a platform to create thermal counterparts of electronic devices, we delve into the study of stochastic behavior of thermal transistors. As devices continue to shrink, the impact of fluctuations becomes an eminent feature, and it may offer insight into different properties in the system [13,14]. While there can be inherent fluctuations due to thermal noise, they can also occur as a result of an external disturbance to the environment, such as a measurement. Characterizing such stochastic behavior may provide an understanding of the limitations in the operation of small-scale devices. Hence, establishing a stochastic description for existing thermal transistor models becomes an important analysis. The absence of an equivalent to a small signal or noise model as in an electronic transistor limits the understanding of its diversion from average behavior. To address this challenge, this paper presents a framework to study the stochastic behavior of a thermal transistor under continuous measurements, providing notable insight for its future implementation. This field of stochastic thermal machines is still evolving, with foundations laid by the researchers in Refs. [15–19]. We anticipate that our modeling and ongoing research in quantum electrodynamics [20], charge transport [21], Floquet engineering [22,23], metamaterials [24], nanoparticles [25], superconducting circuits [26,27], and spasers [28] will contribute to the physical implementation of quantum devices for various purposes influenced by electronics in future.

In our earlier transistor models [5,7,10,12], we obtain a master equation using the reduced dynamics method [29]. This approach, however, masks the changes to the system when coupled with environments that undergo interference. Hence, in this paper, we use an alternative approach drawn from the works in Refs. [16,30–32], known as the quantum trajectory method, where we establish a stochastic description before deriving the average dynamics. Going back to the transistor model, it comprises three thermal baths of distinct temperatures that can carry away information about the system. According to the literature, it is possible to use a detector to obtain this information by measuring the baths. There are two types of such measurements: a selective

*uthpala.ekanayake@monash.edu
†malin.premaratne@monash.edu

measurement and a nonselective measurement. The detector retains no information about its measurement records in a nonselective measurement. Conversely, the detector keeps track of its measurement records in a selective measurement. As it keeps on recording, the states of the system change, and this gets represented in the stochastic Schrödinger equation (SSE). The solutions to the SSE are called quantum trajectories that describe the system's time-dependent state conditioned on the monitoring [13,29]. The ensemble of such trajectories unravels the conditioned master equation. This includes the stochastic components, facilitating examining stochastic properties within a complex system. If the detector cannot extract all the information from the baths, we describe the measurement as inefficient [13].

In this paper, we use the concept of continuous monitoring, a selective but weak measurement scheme [29,33,34], to study the transistor behavior under quantum and environmental fluctuations. The study in Ref. [35] identifies that continuous monitoring can modify energy transport in a nanoscale device. This weak measurement changes the state of the system but also reveals partial information about it. The authors achieve this by treating a zero-temperature bath as a measuring probe that continuously monitors the system. They use Born-Markov approximations in the master equation with additive contributions from the interactions between the system, thermal baths, and the measurement probe. Further, Ref. [36], presents a Brownian thermal transistor in a mesoscopic system to understand quantum transport with fluctuations. Inspired by these works, we develop a stochastic description for a thermal transistor under environmental disturbances. The three terminals of our transistor modeled using two-level systems (TLSs), each connected to three thermal baths with nonzero temperatures, are monitored via three detectors. We consider a continuous monitoring of the baths with weak measurements that partially carry away information about the system. Engineering the baths with a calorimetric ability, rather than the separate detectors, is also a possibility. We provide only a brief elaboration of an experimental setup as our main intention is to study only its impact in a substantial level. The closest experimental setup is to couple the TLSs/transistor terminals to a quantum field that interacts with bath modes with known amplitude and phase. The shift in the frequency of the field can then be approximated as a relaxation occurring in the system, which gets detected by a separate detector or the engineered baths. This can be similar to a homodyne measurement. For interested readers, similar measurement techniques are discussed in Refs. [33,37,38] for various thermal machines.

Our analysis will pave the way for an improved model for a thermal management system under environment monitoring. We commence our analysis by referring to the works in Refs. [39–42]. We establish a diffusion-type quantum trajectory since our model involves nonzero bath temperatures [43]. This is based on the weak measurements of the environment after each of its interactions with the system. We also consider that the baths are in the Ohmic region and the transistor is operating in a limit delivering white noise. Hence, an uncorrelated white noise gets introduced into the system as a Wiener increment each time a measurement channel opens. Finally, we produce a numerical solution for the transistor dynamics based on Euler-Maruyama approximation [44].

We organize our work in this paper as follows. In Sec. II, we describe the stochastic behavior and the transistor model, followed by subsections defining the stochastic master equation for the thermal transistor, noise sources, spectral density representation, and the formation of stochastic energy flows in the system. In Sec. III, we visualize our results, closing with conclusions and limitations in Sec. IV.

II. FORMALISM

A. Stochastic behavior and the quantum trajectory

It is possible to observe the stochastic nature in transistor dynamics when the thermal baths serve as noise sources, reflected in dissipation rates denoted by $\gamma_{\rm P}(\omega)$ (Sec. II D). We extend this framework to encompass a stochastic nature in the description of energy exchange, considering measurements. A stochastic process can be formulated in an open quantum system using the open system's wave function [13,45–47]. The basis here is that a measurement describes the evolution of this wave function [48]. The stochastic representation of a Markovian process can be described using a quantum trajectory, which is the solution to the stochastic master equation (SME) evolving via a continuous measurement [29,49]. Heat flow is presumed to obey a diffusion equation and can be regarded as the continuum limit of a discrete random walk [50]. Also, at positive temperatures, only diffusive terms are applicable [43]. Hence, we start our discussion with an evolution for a diffusive quantum trajectory r, whose states are represented by $\overline{\rho}_r$, similar to the one described in Ref. [51] (for the derivation of this trajectory, refer to Appendix B):

$$\begin{aligned} \mathrm{d}\overline{\rho}_r(t) = &-\frac{i}{\hbar}[\hat{H}, \overline{\rho}_r(t)]\mathrm{d}t + \mathcal{L}[\overline{\rho}_r(t)]\mathrm{d}t + \sqrt{\gamma_\uparrow}[\hat{\sigma}^-\overline{\rho}_r(t) + \overline{\rho}_r(t)\hat{\sigma}^+ - (\langle\hat{\sigma}^-\rangle\overline{\rho}_r(t) + \overline{\rho}_r(t)\langle\hat{\sigma}^+\rangle)]\mathrm{d}W_1^r(t) \\ &+ \sqrt{\gamma_\downarrow}[\sigma^+\overline{\rho}_r(t) + \overline{\rho}_r(t)\hat{\sigma}^- - (\langle\hat{\sigma}^+\rangle\overline{\rho}_r(t) + \overline{\rho}_r(t)\langle\hat{\sigma}^-\rangle)]\mathrm{d}W_2^r(t), \end{aligned} \tag{1}$$

where

$$\mathcal{L}[\overline{\rho}_r(t)] = \gamma_\uparrow\big(\hat{\sigma}^-\overline{\rho}_r(t)\hat{\sigma}^+ - \tfrac{1}{2}\{\hat{\sigma}^+\hat{\sigma}^-, \overline{\rho}_r(t)\}\big) + \gamma_\downarrow(\hat{\sigma}^+\overline{\rho}_r(t)\hat{\sigma}^- - \tfrac{1}{2}\{\hat{\sigma}^-\hat{\sigma}^+, \overline{\rho}_r(t)\}\big). \tag{2}$$

Here, $\hat{\sigma}^-$ and $\hat{\sigma}^+$ represent the system operators that interact with a thermal bath, and $\hat{H}$ is the TLS Hamiltonian (see Appendix A). Also, $\langle\hat{\sigma}^+\rangle$ and $\langle\hat{\sigma}^-\rangle$ represent the expected values of the system operators (see Appendix B).

Moreover, dW_1^r and dW_2^r represent Weiner increments that satisfy $dW_1^r dW_2^r = \delta_{12} dt$, with δ representing the Kronecker delta. The Weiner increments correspond to noise introduction, for each measurement channel in each time increment dt [37]. The dissipation rates are represented as $\gamma_\uparrow = \mathcal{J}(\omega)[1 + N(\omega)]$, and $\gamma_\downarrow = \mathcal{J}(\omega)N(\omega)$. Here, $\mathcal{J}(\omega)$ corresponds to the spectral density function of the thermal bath, and $N(\omega)$ corresponds to the population of harmonic oscillator mode with frequency ω in a thermal bath with temperature T approximated by the Planck distribution $N(\omega) = \{\exp(\frac{\hbar\omega}{k_B T}) - 1\}^{-1}$ [5], respectively. Note that Eq. (1) generates two measurement records. We describe them as

$$dy_1 = \sqrt{\gamma_\uparrow}\langle\hat{\sigma}^-\rangle dt + dW_1(t),$$
$$dy_2 = \sqrt{\gamma_\downarrow}\langle\hat{\sigma}^+\rangle dt + dW_2(t). \tag{3}$$

In this paper, our interests are in analyzing the impact of measurements on transistor dynamics, as such records get detected in the environment. In a separate study, we will investigate how we can use these measurement records to realize feedback control in thermal transistors. While this feedback control will have different characteristics and outcomes from electronic feedback, we wanted to explore how control can help preserve quantum coherence that can be used to realize a dark state [12] as a targeted state. Next, we approximate Eq. (1) to an evolution produced by a single measurement channel. We follow Refs. [14,51,52], to obtain an approximate measurement resembling a homodyne measurement. Further elaboration on this is in Appendix B. We now use a stochastic evolution as follows for an ensemble of quantum trajectories ρ_r as

$$d\rho_r(t) = -\frac{i}{\hbar}[\hat{H}, \rho_r(t)]dt + \mathcal{L}[\rho_r(t)]dt + \sqrt{\frac{\mathcal{J}(\omega)\zeta}{1+2N(\omega)}}[1+N(\omega)]\{\sigma^-\rho_r(t) + \rho_r(t)\sigma^+ - [\langle\sigma^-\rangle\rho_r(t) + \rho_r(t)\langle\sigma^+\rangle]\}dW^r$$
$$+ \sqrt{\frac{\mathcal{J}(\omega)\zeta}{1+2N(\omega)}}[-N(\omega)]\{\sigma^+\rho_r(t) + \rho_r(t)\sigma^- - [\langle\sigma^+\rangle\rho_r(t) + \rho_r(t)\langle\sigma^-\rangle]\}dW^r. \tag{4}$$

with, $\zeta \in [0, 1]$ controlling the efficiency of the measurement. Note that the quantum state ρ_r differs from the previous system state $\overline{\rho}_r$ as the observer's knowledge about the system is now imperfect [52]. However, we visualize that even under these new states, by appropriately tuning ζ for weak measurements, we can preserve the transistor dynamics. Now, we extend this behavior for a transistor model consisting of three TLSs, as in Fig. 1. It consists of three TLSs as terminals, each interacting with three baths with temperatures T_L, T_M, and T_R. Three detectors are placed to monitor the three baths continuously.

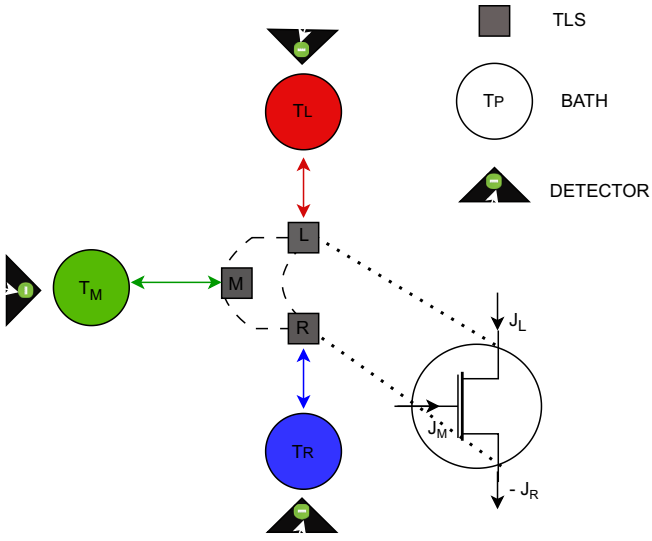

FIG. 1. Transistor arrangement with three TLSs as terminals interacting with reservoirs B_L, B_M, and B_R, each with temperatures T_L, T_M, and T_R. The interactions of baths with TLSs are shown in solid lines. The three detectors that monitor the baths are also shown. The three energy flows at steady state, J_L, J_M, and J_R, are marked in the diagram.

B. System description

The system Hamiltonian $\hat{H}_{\text{sys}}$ takes the following form (as in previous models [7,12]) :

$$\hat{H}_{\text{sys}} = \frac{\hbar}{2}\big(\omega_L\hat{\sigma}_L^z + \omega_M\hat{\sigma}_M^z + \omega_R\hat{\sigma}_R^z + \omega_{LM}\hat{\sigma}_L^z\hat{\sigma}_M^z + \omega_{MR}\hat{\sigma}_M^z\hat{\sigma}_R^z + \omega_{RL}\hat{\sigma}_R^z\hat{\sigma}_L^z\big). \tag{5}$$

Here, $\hbar\omega_{\text{P}}$ is the energy difference between the two eigenstates of the TLS P, $\hbar$ representing the reduced Planck constant. Moreover, $\hbar\omega_{\text{PQ}}^s$ is the interaction energy between a pair of TLSs, P and Q (P, Q $\in \{L, M, R\}$). Furthermore, $\hat{\sigma}_{\text{P}}^z$ are the expanded Pauli matrices representing the compound system. The Hamiltonian of the baths takes the form [53]

$$\hat{H}_{\text{bath}}^{\text{P}} = \sum_k \hbar\omega_k^{\text{P}}\,\hat{b}_k^{\text{P}\,\dagger}\hat{b}_k^{\text{P}}, \tag{6}$$

with $\hat{b}_k^{\text{P}}$ representing the annihilation operator for a bath mode ω_k. The system-bath interaction Hamiltonian follows:

$$\hat{H}_{\text{sys-bath}}^{\text{P}} = \hbar\hat{\sigma}_{\text{P}}^x \otimes \sum_k g_k^{\text{P}}\big(\hat{b}_k^{\text{P}} + \hat{b}_k^{\text{P}\dagger}\big), \tag{7}$$

with g_k^{P} representing the coupling constant between TLS P and the operators in bath P. Hence, the total Hamiltonian $\hat{H}_{\text{T}}$ of the transistor describes:

$$\hat{H}_{\text{T}} = \hat{H}_{\text{sys}} + \sum_{\text{P}\in\{L,M,R\}}\big(\hat{H}_{\text{bath}}^{\text{P}} + \hat{H}_{\text{sys-bath}}^{\text{P}}\big). \tag{8}$$

C. Stochastic master equation for the thermal transistor (three strongly coupled TLSs)

Now, we derive the stochastic master equation for three strongly coupled TLSs, which are in contact with three heat baths with distinct temperatures, undergoing weak continuous measurements [39]. A quantum trajectory of a single TLS coupled to a bath undergoing continuous measurement follows Eq. (4). Thus, we replace the system operators $\sqrt{\gamma_\uparrow}\sigma_{\rm P}^-$ and $\sqrt{\gamma_\downarrow}\sigma_{\rm P}^+$ with $\sqrt{\mathcal{J}_{\rm P}(\omega)[1+N_{\rm P}(\omega)]}\hat{A}_{\rm P}(\omega)$ and $\sqrt{\mathcal{J}_{\rm P}(\omega)N_{\rm P}(\omega)}\hat{A}_{\rm P}^\dagger(\omega)$, P $\in \{L, M, R\}$ respectively to suit our transistor system. Here,

$$\mathcal{J}_{\rm P}(\omega) = \sum_k 2\pi \left|g_k^{\rm P}\right|^2 \delta(\omega - \omega_k). \tag{9}$$

For this transistor model we take this function to be Ohmic [5], and use a modeling constant $\kappa_{\rm P}$ [54] to represent the thermal bath spectral density as

$$\mathcal{J}_{\rm P}(\omega) = \kappa_{\rm P}\omega. \tag{10}$$

And also,

$$\hat{A}_{\rm P}(\omega) = \sum_{\epsilon'-\epsilon=\hbar\omega} |\epsilon\rangle\langle\epsilon|\sigma_{\rm P}^x|\epsilon'\rangle\langle\epsilon'|, \tag{11}$$

where we decompose the system Hamiltonian as $\hat{H}_{\rm sys} = \sum_i \epsilon_i|\epsilon_i\rangle\langle\epsilon_i|$. We select $\hat{H}_{\rm sys}$ that is already diagonalizable in the bare states. Hence, the first term vanishes as there is no Hamiltonian evolution. Then, we arrive at Eq. (12) from Eq. (4) that represents the stochastic master equation for the transistor system, for a realization r. (for a detailed derivation refer to Appendix B):

$$\mathrm{d}\rho_r(t) = \sum_{{\rm P}\in(L,M,R)} \mathcal{L}_{\rm P}[\rho_r(t)]\mathrm{d}t + \sum_{{\rm P}\in(L,M,R)} \mathcal{M}_{\rm P}[\rho_r(t)]\mathrm{d}W_{\rm P}^r(t), \tag{12}$$

where

$$\mathcal{L}_{\rm P}[\rho_r(t)] = \sum_{\omega>0}\Bigg[\mathcal{J}_{\rm P}(\omega)[1+N_{\rm P}(\omega)]\left(\hat{A}_{\rm P}(\omega)\rho_r(t)\hat{A}_{\rm P}^\dagger(\omega) - \frac{1}{2}\{\hat{A}_{\rm P}^\dagger(\omega)\hat{A}_{\rm P}(\omega), \rho_r(t)\}\right) + \mathcal{J}_{\rm P}(\omega)N_{\rm P}(\omega)\left(\hat{A}_{\rm P}^\dagger(\omega)\rho_r(t)\hat{A}_{\rm P}(\omega) - \frac{1}{2}\{\hat{A}_{\rm P}(\omega)\hat{A}_{\rm P}^\dagger(\omega), \rho_r(t)\}\right)\Bigg] \tag{13}$$

and

$$\mathcal{M}_{\rm P}[\rho_r(t)] = \sum_\omega \sqrt{\frac{\mathcal{J}_{\rm P}(\omega)\zeta}{1+2N_{\rm P}(\omega)}}[1+N_{\rm P}(\omega)](\hat{A}_{\rm P}(\omega)\rho_r(t) + \rho_r(t)\hat{A}_{\rm P}^\dagger(\omega) - [\langle\hat{A}_{\rm P}(\omega)\rangle\rho_r(t) + \rho_r(t)\langle\hat{A}_{\rm P}^\dagger(\omega)\rangle]) + \sum_\omega \sqrt{\frac{\mathcal{J}_{\rm P}(\omega)\zeta}{1+2N_{\rm P}(\omega)}}[-N_{\rm P}(\omega)](\hat{A}_{\rm P}^\dagger(\omega)\rho_r(t) + \rho_r(t)\hat{A}_{\rm P}(\omega) - [\langle\hat{A}_{\rm P}^\dagger(\omega)\rangle\rho_r(t) + \rho_r(t)\langle\hat{A}_{\rm P}(\omega)\rangle]) . \tag{14}$$

Here, $\mathrm{d}W_{\rm P}^r(t)$ represents the Wiener increments, with a Wiener process having zero mean and $\mathrm{d}t$ variance. Next, we need a numerical method to solve $\rho_r(t)$. We first find the Ito-Taylor expansion of $\rho_r(t)$, and then consider its Euler-Maruyama approximation as described in Refs. [44,55]. For a particular realization r, we expand the solution for the state dynamics as

$$\rho_r(t+\Delta t) = \rho_r(t) + \sum_{{\rm P}\in(L,M,R)} \mathcal{L}_{\rm P}[\rho_r(t)]\Delta t + \sum_{{\rm P}\in(L,M,R)} \mathcal{M}_{\rm P}[\rho_r(t)]\Delta W_{\rm P}^r(t) + \frac{1}{2}\sum_{{\rm P}\in(L,M,R)} \mathcal{M}_{\rm P}^2[\hat{\rho}(t)]\left[\Delta W_{\rm P}^{2,r}(t) - \Delta t\right] + \tilde{R}. \tag{15}$$

Here, $\tilde{R}$ represents

$$\tilde{R} = \sum_{{\rm P}\in(L,M,R)}\Bigg(\int_{t_0}^t\int_{t_0}^{\tau_1} L_{\rm P}^0\mathcal{L}_{\rm P}[\rho_r(\tau_2)]\,\mathrm{d}\tau_2\,\mathrm{d}\tau_1 + \int_{t_0}^t\int_{t_0}^{\tau_1} L_{\rm P}^1\mathcal{L}_{\rm P}[\rho_r(\tau_2)]\,\mathrm{d}W_{\rm P}^r(\tau_2)\,\mathrm{d}\tau_1 + \int_{t_0}^t\int_{t_0}^{\tau_1} L_{\rm P}^0\mathcal{M}_{\rm P}[\rho_r(\tau_2)]\,\mathrm{d}\tau_2\,\mathrm{d}W_{\rm P}^r(\tau_1) + \int_{t_0}^t\int_{t_0}^{\tau_1}\int_{t_0}^{\tau_2} L_{\rm P}^0L_{\rm P}^1\mathcal{M}_{\rm P}[\rho_r(\tau_3)]\,\mathrm{d}\tau_3\,\mathrm{d}W_{\rm P}^r(\tau_2)\,\mathrm{d}W_{\rm P}^r(\tau_1) + \int_{t_0}^t\int_{t_0}^{\tau_1}\int_{t_0}^{\tau_2} L_{\rm P}^1L_{\rm P}^1\mathcal{M}_{\rm P}[\rho_r(\tau_3)]\,\mathrm{d}W_{\rm P}^r(\tau_3)\,\mathrm{d}W_{\rm P}^r(\tau_2)\,\mathrm{d}W_{\rm P}^r(\tau_1)\Bigg), \tag{16}$$

where we define linear operators such that

$$L_{\rm P}^0\mathcal{G}_P[X] = \mathcal{L}_{\rm P}[X]\frac{\partial}{\partial X}\mathcal{G}_P[X] + \frac{1}{2}\mathcal{M}_{\rm P}^2[X]\frac{\partial^2}{\partial X^2}\mathcal{G}_P[X],$$
$$L_{\rm P}^1\mathcal{G}_P[X] = \mathcal{M}_{\rm P}[X]\frac{\partial}{\partial X}\mathcal{G}_P[X], \tag{17}$$

for any function $\mathcal{G}_P[X]$. We consider Δt long compared to the reservoir memory time τ_c but short compared to the relaxation time of the system τ_R. Applying the Euler approximation [29], Eq. (15) reduces to

$$\rho_r(t+\Delta t) \approx \rho_r(t) + \sum_{\mathrm{P}\in(L,M,R)} \mathcal{L}_{\mathrm{P}}[\rho_r(t)]\Delta t + \sum_{\mathrm{P}\in(L,M,R)} \mathcal{M}_{\mathrm{P}}[\rho_r(t)]\Delta W_{\mathrm{P}}^r(t). \quad (18)$$

This is similar to the technique used in deriving the small-signal model for an electronic transistor, where we approximate a nonlinear function by its first-order derivatives. The density matrix, which is the ensemble average of the system, can be reproduced from the expectation value of the stochastic ensemble [29,56,57] as

$$\mathrm{d}\hat{\rho} \equiv \langle \mathrm{d}\rho_r \rangle_r, \quad (19)$$

which removes the Wiener increments. Thus, we unravel the quantum master equation

$$\frac{\mathrm{d}\hat{\rho}(t)}{\mathrm{d}t} = \sum_{\mathrm{P}\in(L,M,R)} \mathcal{L}_{\mathrm{P}}[\hat{\rho}(t)]. \quad (20)$$

This shows that monitoring the baths prompts to similar system dynamics when ignored the results of the monitoring [13].

D. Noise representation

We model the thermal baths, which act as the primary noise source in the system, using Eq. (6). The bath operators $\hat{b}_k^{\mathrm{P}}$ hence contribute to the inherent noise in the system. We describe a separate noise operator for each bath $\mathrm{P} \in \{L, M, R\}$ as

$$\hat{B}_{\mathrm{P}}(t) = g_k^{\mathrm{P}}\left(e^{-i\omega_k t}\hat{b}_k^{\mathrm{P}} + e^{i\omega_k t}\hat{b}_k^{\mathrm{P}\dagger}\right). \quad (21)$$

We now use the fluctuation-dissipation theorem to analyze the transistor system behavior to small perturbations [58–60] due to their connection to thermal baths. These baths are the main source of noise in the system [8], apart from the measurement noise that gets introduced. The measurement noise can relate to the Wiener increments and is treated as shot noise in Ref. [61] as long as there is an interface between the measurement and its detection. In our case, we term this as a measurement noise as we do not elaborate on such an interface. In this section, we explore thermal noise and express thermal noise power $S_{\mathrm{P}}(\omega)$ for each bath P, by considering the correlation of the bath operators [62] as

$$S_{\mathrm{P}}(\omega) = \int_{-\infty}^{\infty} e^{i\omega\tau}\mathrm{Tr}_B[\hat{B}_{\mathrm{P}}^{\dagger}(t)\hat{B}_{\mathrm{P}}(t-\tau)\rho_B]\,\mathrm{d}\tau = \gamma_{\mathrm{P}}(\omega). \quad (22)$$

with ρ_B representing bath thermal state, and Tr_B representing the partial trace over the bath. The noise power $S_{\mathrm{P}}(\omega)$ is equal to the dissipation rate of the system $\gamma_{\mathrm{P}}(\omega)$, which is the two-sided Fourier transform of the bath correlation function [54]. We take ω to represent all the transition frequencies happening between the energy levels of the system. Let us simplify the bath correlation by taking the baths mode as ω_k:

$$\begin{aligned}\mathrm{Tr}_B[B_{\mathrm{P}}^{\dagger}(t)B_{\mathrm{P}}(t-\tau)\hat{\rho}_B] &= \langle B_{\mathrm{P}}^{\dagger}(t)B_{\mathrm{P}}(t-\tau)\rangle \\ &= \left|g_k^{\mathrm{P}}\right|^2\left(e^{-i\omega_k\tau}\langle \hat{b}_k^{\mathrm{P}}\hat{b}_k^{\mathrm{P}\dagger}\rangle + e^{i\omega_k\tau}\langle \hat{b}_k^{\mathrm{P}\dagger}\hat{b}_k^{\mathrm{P}}\rangle\right) \\ &= \left|g_k^{\mathrm{P}}\right|^2(e^{-i\omega_k\tau}[1+N_{\mathrm{P}}(\omega_k)] + e^{i\omega_k\tau}N_{\mathrm{P}}(\omega_k)). \end{aligned} \quad (23)$$

Note that

$$\begin{aligned}\langle \hat{b}_k^{\mathrm{P}}\hat{b}_k^{P\dagger}\rangle &= N_{\mathrm{P}}(\omega_k), \\ \langle \hat{b}_k^{\mathrm{P}\dagger}\hat{b}_k^{\mathrm{P}}\rangle &= [1+N_{\mathrm{P}}(\omega_k)]. \end{aligned} \quad (24)$$

Hence, Eq. (22) simplifies to

$$\gamma_{\mathrm{P}}(\omega) = \sum_k 2\pi\left|g_k^{\mathrm{P}}\right|^2\{N_{\mathrm{P}}(\omega)\delta(\omega+\omega_k) + [1+N_{\mathrm{P}}(\omega)]\delta(\omega-\omega_k)\}. \quad (25)$$

The spectral density of the thermal bath takes the form in Eq. (9). For this transistor model, we introduce κ_{P} to represent an Ohmic thermal bath spectral density as in Eq. (10). Therefore, we represent the noise spectral density function in Eq. (25) as

$$\gamma_{\mathrm{P}}(\omega) = \kappa_{\mathrm{P}}\omega[N_{\mathrm{P}}(\omega) + (1+N_{\mathrm{P}}(\omega))] = \gamma_{\uparrow} + \gamma_{\downarrow}. \quad (26)$$

In the low frequency limit, we represent

$$N_{\mathrm{P}}(\omega) \approx 1 + N_{\mathrm{P}}(\omega) = \frac{k_{\mathrm{B}}T_{\mathrm{P}}}{\hbar\omega}, \quad (27)$$

where, k_{B} is the Boltzmann constant. Hence, we express the noise power for the bath as

$$\gamma_{\mathrm{P}}(\omega) = 2\left(\frac{\kappa_{\mathrm{P}}}{\hbar}\right)k_{\mathrm{B}}T_{\mathrm{P}}. \quad (28)$$

The spectral density exhibits a uniform response to low frequencies, similar to Johnson-Nyquist noise. This noise is inherently present in the system, and we quantify it using $(\frac{\kappa_{\mathrm{P}}}{\hbar})$. We represent this in Fig. 2. Notably, this parameter is directly related to the dissipation rate, $\gamma_{\mathrm{P}}(\omega)$ at bath temperature T_{P}.

Now, let us discuss the input noise modeling during the measurements. Quantum noise can get introduced to the system during measurement via any noisy input field. We can represent this kind of noise as $\mathrm{d}\hat{B}_{\mathrm{in}} = \hat{b}_{\mathrm{in}}\mathrm{d}t$ [30,56,63]. Here,

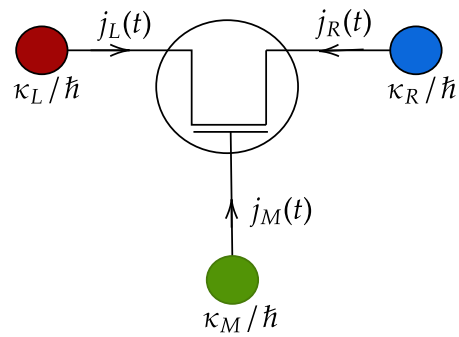

FIG. 2. A thermal transistor representing noise from baths as $(\frac{\kappa_L}{\hbar})$, $(\frac{\kappa_M}{\hbar})$, and $(\frac{\kappa_R}{\hbar})$, and the fluctuating energy flows as $j_L(t)$, $j_M(t)$, and $j_R(t)$ due to continuous monitoring of baths.

$\hat{b}_{\text{in}}$ can be a bath operator in a vacuum state that interacts with the system. This noise component satisfies

$$\langle \mathrm{d}\hat{B}_{\text{in}}(t)\rangle = 0,$$
$$\mathrm{d}\hat{B}_{\text{in}}(t)\mathrm{d}\hat{B}^{\dagger}_{\text{in}}(t) = \mathrm{d}t. \tag{29}$$

In our model, we generalize this representation using a Wiener process having the same properties. Let us introduce noise given by $\varepsilon_{\text{P}}(t,\omega)$ for all transition frequencies ω between the energy levels happening in the system due to bath P interaction. Hence, we define a real-valued Wiener process

$$W_{\text{P}}(t,\omega) = \int_{t_0}^{t} \varepsilon_{\text{P}}(t',\omega)\,\mathrm{d}t', \tag{30}$$

in order to model the noise introduction to the system, as per the Lax developments [52]. In Eq. (18), $\Delta W_{\text{P}}(t) \equiv \Delta W_{\text{P}}(t,\omega)$, representing a Wiener increment,

$$\Delta W_{\text{P}}(t,\omega) = W_{\text{P}}(t+\Delta t,\omega) - W_{\text{P}}(t,\omega), \tag{31}$$

with Δt as the variance, defined for all the transitions. These increments satisfy the conditions $\sum_{\omega}\langle \Delta W_{\text{P}}(t,\omega)\rangle = 0$ and $\sum_{\omega}\Delta W^2_{\text{P}}(t,\omega) = \Delta t$. Note that we handle Eq. (12) with efficiency thresholds based on bath phonon distribution as discussed in Appendix B, to introduce noise from baths in thermal states during a measurement. This noise input hence results in fluctuating energy flow components in Eq. (34).

E. Energy flows at steady state

According to Ref. [35], the total energy flow J_P from the baths into the system as in the thermal transistor relates to

$$\begin{aligned}\sum_{\text{P}\in(L,M,R)} J_{\text{P}}(t) &= \frac{\partial\langle \hat{H}_{\text{sys}}\rangle}{\partial t}\\ &= \mathrm{Tr}\left\{\hat{H}_{\text{sys}}\frac{\mathrm{d}\hat{\rho}(t)}{\mathrm{d}t}\right\}\\ &= \mathrm{Tr}\left\{\hat{H}_{\text{sys}}\left\langle\frac{\mathrm{d}\rho_r(t)}{\mathrm{d}t}\right\rangle_r\right\}\\ &= \sum_{\text{P}\in(L,M,R)}\mathrm{Tr}\{\hat{H}_{\text{sys}}\langle\mathcal{L}_{\text{P}}[\rho_r(t)]\rangle_r\}\\ &\quad+\sum_{\text{P}\in(L,M,R)}\mathrm{Tr}\left\{\hat{H}_{\text{sys}}\left\langle\mathcal{M}_{\text{P}}[\rho_r(t)]\frac{\Delta W^r_{\text{P}}}{\Delta t}\right\rangle_r\right\},\end{aligned} \tag{32}$$

with Tr denoting the matrix trace. Let us call $J_P(t)$ the stochastic energy flow in the system. Here, the first term

$$\overline{J}_{\text{P}}(t) = \mathrm{Tr}\{\hat{H}_{\text{sys}}\langle\mathcal{L}_{\text{P}}[\rho_r(t)]\rangle_r\} = \mathrm{Tr}\{\hat{H}_{\text{sys}}\mathcal{L}_{\text{P}}[\hat{\rho}(t)]\} \tag{33}$$

corresponds to the average heat flow in the system. Furthermore, the second term

$$j_{\text{P}}(t) = \mathrm{Tr}\left\{\hat{H}_{\text{sys}}\left\langle\mathcal{M}_{\text{P}}[\rho_r(t)]\frac{\Delta W^r_{\text{P}}}{\Delta t}\right\rangle_r\right\} \tag{34}$$

represents the fluctuating energy component. Note that for a collection of realizations, with no coherence terms in the steady states, this fluctuating energy component $\mathrm{Tr}\{\hat{H}_{\text{sys}}\langle\mathcal{M}_{\text{P}}[\rho_r]\frac{\Delta W^r_{\text{P}}}{\Delta t}\rangle_r\} = 0$. The analysis in Ref. [34] treats this as a measurement work due to the monitoring from the detectors. As Eq. (32) consists of two components, the average energy flow and a time-varying element that has an average of zero at a steady state, the energy flow restricts to perturbations about an operating point, resembling the behavior of an electronic transistor small-signal model. Even though stochastic Schrödinger equations are nonlinear, we can approximate that to express a linear behavior for the system. Hence, just like the small-signal model used in electronics, our model is applicable within a narrow range controlled by ζ, around an operating point, that delivers average energy across the system. Nevertheless, these models can still be useful to get an insight when employed beyond their specified range of validity [64].

III. RESULTS AND DISCUSSION

We compare the average dynamics with the reduced density matrix approach to validate our results. The importance of the quantum trajectory method is that it gives insight into the occurrence of fluctuation in the energy flow. We use *Mathematica* V12 to simulate the stochastic process of the model. We visualize the transistor model energy flow under weak continuous measurements (please refer to Supplemental Material [65] for the associated code). We consider a scenario with the following parameters, consistent with the studies in Refs. [5,12]: $\omega_L = 0.05\Delta$, $\omega_M = 0.1\Delta$, $\omega_R = 0$, $\omega_{LM} = \Delta$, $\omega_{MR} = \Delta$, $\omega_{RL} = 0$, $\kappa_{\text{P}} = 0.01$, $T_L = 0.2T$, $T_M = 0.1T$, and $T_R = 0.02T$, with Δ and T as scaling factors that can incorporate units or change the operation range of the transistor. If one is working in SI units, $\Delta = 1.3\times10^{11}$ Hz and $T = 0.5$ mK. For computational simplicity and to reduce memory and simulation time with the given computer capacity, we

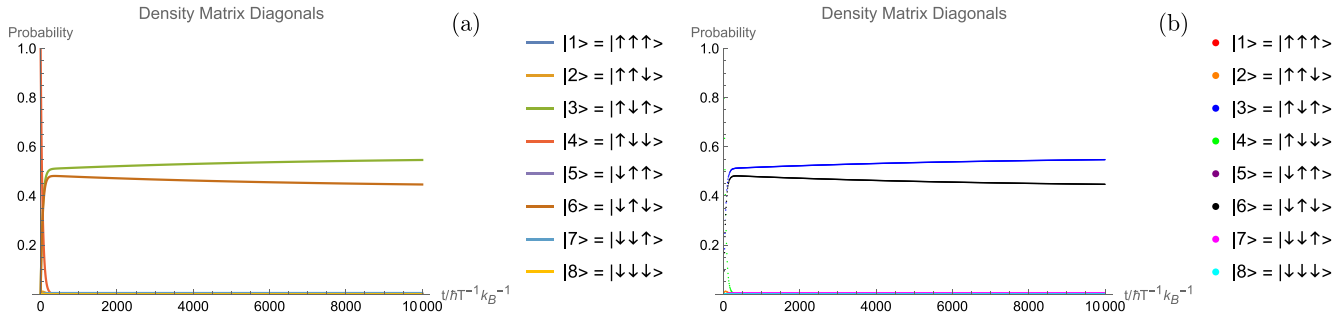

FIG. 3. Transistor dynamics from (a) reduced density matrix approach and (b) using the quantum trajectory method.

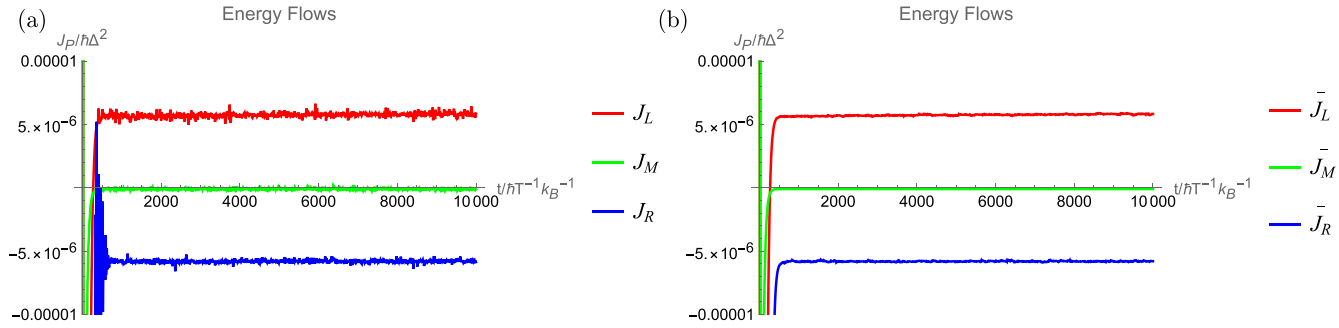

FIG. 4. (a) The stochastic energy flows $J_L(t)$, $J_M(t)$, and $J_R(t)$ from the baths for 100 realizations, keeping $\zeta = 0.02$, and (b) average energy flows $\bar{J}_L$, $\bar{J}_M$, and $\bar{J}_R$.

work in normalized units. In the trajectory method, we limit $0 < \zeta < 0.1$, to specify the range of validity that will not change the original transistor action excessively, and keep the energy flow variation with temperature approximately linear up-to a certain temperature limit. Accordingly, in Fig. 3, we obtain similar transistor states at the steady state when using both methods. The average dynamics of the quantum trajectory method delivers the same transistor states. Hence, this approach is suitable for implementing a new transistor model for the existing thermal transistor that considers external disturbances to the environment such as a measurement. Next, we visualize how the energy flow varies in the new model with time. Figure 4 gives a comparison in timescale of a visualization of stochastic energy flow and the average energy flow without continuous monitoring ($\zeta = 0$).

The energy flow has fluctuations with time when we consider the continuous disturbances to the bath. With no monitoring, these fluctuations subside, giving the average energy flow. Next, we visualize how the energy flows from the trajectory method at a steady state vary with the control bath temperatures T_M as in Fig. 5. We make a comparison of this variation with the average energy flow without continuous monitoring. Note that the stochastic energy flow and the energy flow without monitoring have the same variation at a steady state, with the selected $\zeta = 0.02$.

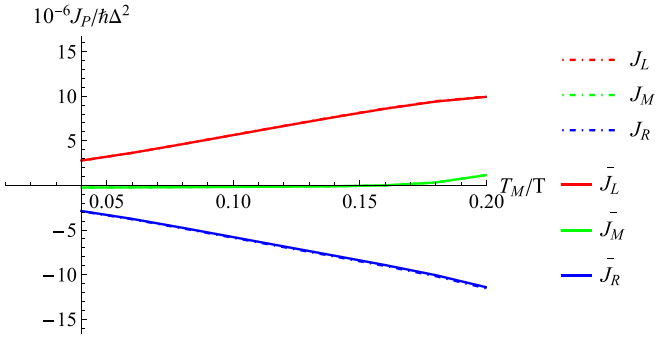

FIG. 5. The average energy flows $\bar{J}_P$ (solid lines) at steady state with no monitoring, and the energy flows at a steady state from the stochastic model J_P (dotted lines) considering 100 realizations, and $\zeta = 0.02$ varying with the control bath temperature T_M. Note that the variation of J_L is approximately linear up to $T_M = 0.15T$, which prompts us to use this gradient to define a new parameter for the model as thermal conductance(c).

The literature provides various transistor parameters to analyze the transistor effect. We first introduce transistor amplification factor α [Eq. (35)] and transistor thermal efficiency β [Eq. (36)]. We compare these values with our conditioned system by varying the measurement efficiency parameter ζ, which significantly changes the conditioning strength under a fixed Ohmic bath constant $\kappa_P = 0.01$, with the original model as outlined in Refs. [2,6]. Equations (35) and (36) are defined for the conditioned thermal transistor under $J_L \approx -J_R$. We select $0 \leqslant \zeta \leqslant 0.09$ to investigate the variations, limiting the drastic change in energy flows J_L and J_R due to the introduction of measurement noise. Under $J_L = -J_R$,

$$\alpha = \left.\frac{\Delta J_L}{\Delta J_M}\right|_{T_L,T_R} = -\left.\frac{\Delta J_R}{\Delta J_M}\right|_{T_L,T_R}, \tag{35}$$

$$\beta = \frac{J_L}{J_M} = -\frac{J_R}{J_M}, \tag{36}$$

where

$$J_P = \mathrm{Tr}\{\hat{H}_{\mathrm{sys}}\mathcal{L}_P[\hat{\rho}]\} + \mathrm{Tr}\left\{\hat{H}_{\mathrm{sys}}\left\langle \mathcal{M}_P[\rho_r]\frac{\Delta W_P^r}{\Delta t}\right\rangle_r\right\}$$

for $P \in \{L, M, R\}$ at a steady state. We visualize these factors by comparing them to an "original model" as in Refs. [2,3]. We notice that the amplification factor remains constant at $\alpha = 40$ within the selected transistor operating range

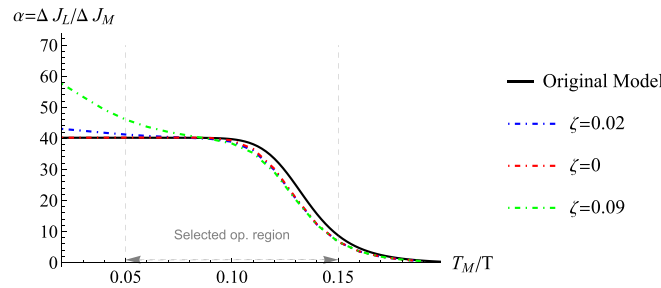

FIG. 6. The amplification factor variation with the original model and changing the noise levels in three cases at a fixed $\kappa_P = 0.01$, by varying ζ at 0, 0.02, and 0.09. The amplification factor usually remains a constant within the selected transistor operating range $0.05T \leqslant T_M \leqslant 0.1T$ for lower levels of noise and then it starts to decrease for $0.1T < T_M \leqslant 0.15T$ with a slightly higher rate when there is conditioning.

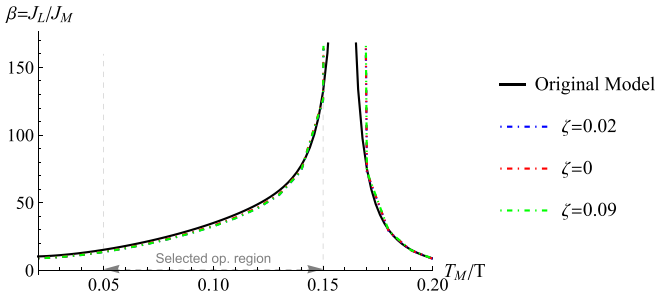

FIG. 7. Thermal efficiency variation with the original model and changing the noise levels in three cases at a fixed $\kappa_{\rm P} = 0.01$, by varying ζ at 0, 0.02, and 0.09. This efficiency factor does not have significant changes in the selected conditioning strengths. It has an increase over our selected transistor operating region $0.05T \leqslant T_M \leqslant 0.15T$, varying between 10 and 130, diverging at $0.16T$ when J_M hits a minimum. Then, it starts to decrease as T_M gets closer to T_L.

$0.05T \leqslant T_M \leqslant 0.1T$ in the original model and in the absence of conditioning. It will remain nearly constant at $\zeta = 0.02$. With an increased ζ, amplification starts to change significantly due to noise (see Fig. 6). Then, α will begin to decrease for $0.1T < T_M \leqslant 0.15T$ for all cases. Even though we see such variations in the amplification with the introduction of noise caused by monitoring, the thermal efficiency β (see Fig. 7) remains nearly the same. This is because of our considered limitations on steady-state energy flows to maintain $J_L \approx -J_R$. Parameter β has an increase over our selected transistor operating region $0.05T \leqslant T_M \leqslant 0.15T$, varying between 10 and 130, and diverging at $0.16T$ when J_M hits a minimum. Afterwards, it starts to decrease as T_M gets closer to T_L. In a separate study, we will discuss how to use continuous monitoring to create feedback and improve these factors.

Let us analyze the rectification factor $R_{M\to L(R)}$ under the heat gradients $T_M > T_{L(R)}$, and $T_M < T_{L(R)}$. We consider the heat flows $J_{M\to L(R)}$ (for $T_M < T_{L(R)}$), and $J_{M\to L(R)}$ (for $T_M > T_{L(R)}$). The concept of the rectification factor is commonly discussed in the context of thermal diodes. Given that an electronic transistor functions as a two-diode system, it is quite natural to analyze this effect. We define thermal rectification

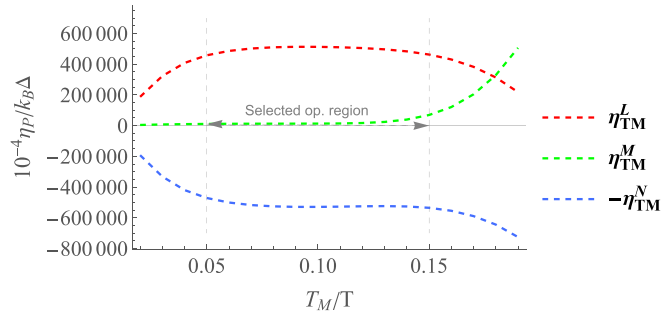

FIG. 9. Thermal sensitivity variation is visualized by changing the control bath temperature. We notice that η^L_{TM} and η^L_{TM} remain nearly constant within the region $0.05T \leqslant T_M \leqslant 0.15T$ and $\eta^M_{TM} \approx 0$. These parameter variations are helpful for establishing a small-signal model in this region.

factor inspired by Refs. [3,66,67] as in Eq. (37),

$$R_{M\to L(R)} = \frac{|J_{L(R)\to M}|}{|J_{M\to L(R)}|}. \tag{37}$$

When $R_{M\to L(R)} = 1$ there is no rectification and when $R_{M\to L(R)} = 0$ there is perfect rectification. As we see in Fig. 8, we observe there is not perfect but some rectification between the input terminal M and L/R terminals for transistor operating region $0.05T \leqslant T_M \leqslant 0.15T$. This rectification variation demonstrates that realizing a quantum thermal transistor with characteristics similar to NPN and PNP diode junctions is a tedious task. Thus, the thermal transistor is not exactly an electronic transistor but it can have similar characteristics showing some rectification.

We now introduce the thermal sensitivity [7,68] to understand how sensitive is the change in the stochastic energy flows to small changes in the control temperature T_M as in Eq. (38). We notice, referring to Fig. 9, that η^L_{TM} and η^R_{TM} remain nearly constant within the region $0.05T \leqslant T_M \leqslant 0.15T$ and $\eta^M_{TM} \approx 0$. These sensitivity variations are why we establish a small-signal model for our thermal transistor:

$$\eta^{\rm P}_{TM} = \frac{\Delta J_{\rm P}}{\Delta T_M}. \tag{38}$$

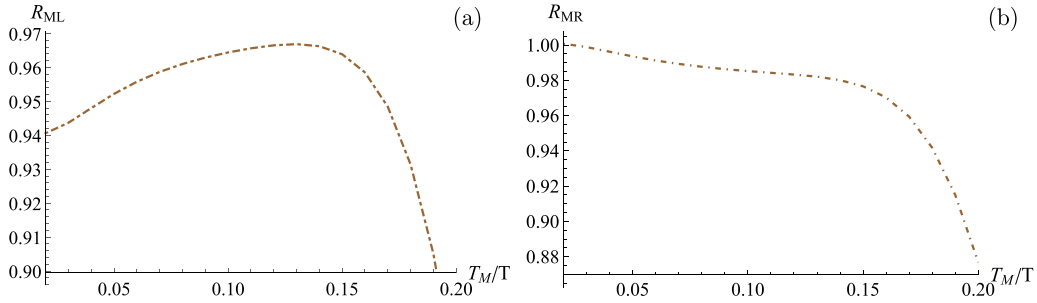

FIG. 8. Transistor rectification factor (a) between terminals M and L ($R_{M\to L}$) and (b) between terminals M and R ($R_{M\to R}$). We observe that there is not perfect but some rectification between the input terminal M and L/R terminals for the transistor operating region. This behavior indicates the challenging nature of achieving a quantum thermal transistor with characteristics exactly similar to those found in NPN and PNP diode junctions. Thus, the thermal transistor is not exactly an electronic transistor but it can have similar characteristics showing some rectification.

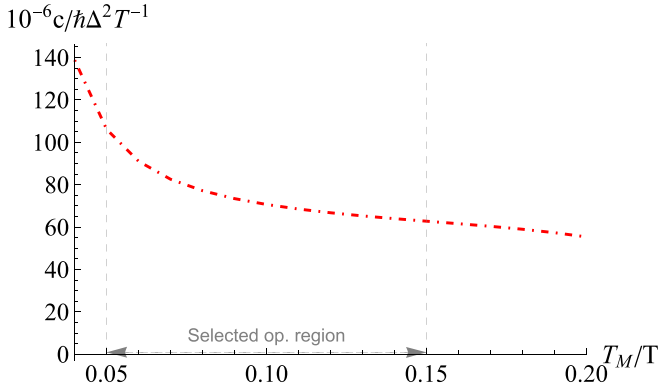

FIG. 10. The diagram expresses the variation of the thermal conductance c between hot and cold baths with the input temperature T_M, keeping temperatures T_L and T_R constant when $\zeta = 0.02$, and $\kappa_P = 0.01$.

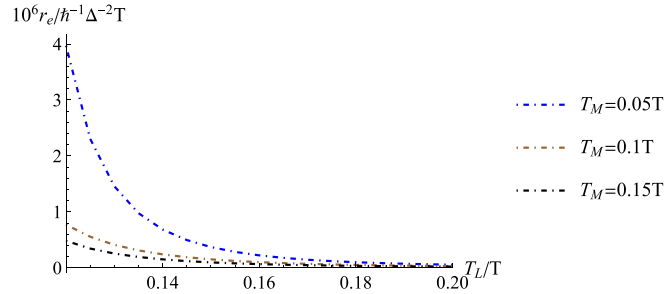

FIG. 11. The diagram expresses the variation in thermal resistance r_e between hot T_L and cold T_R baths at $\zeta = 0.02$ and $\kappa_P = 0.01$, with constant input temperatures $T_M = 0.05T, 0.1T, 0.15T$. Note that as we increase the control temperature T_M the resistance for the heat flow reduces further.

A. Small-signal model

A small-signal model is used in an electronic transistor to analyze how it responds to small variations in its input signal. We obtain a similar model for the quantum thermal transistor by considering the stochastic energy flow from the quantum trajectory approach. With regards to Fig. 5, we notice that $|J_L| \approx |J_R|$ and has an approximately linear increase from $0.05T$ to $0.15T$ and $|J_M| \approx 0$. By referring to Fig. 9, we notice how these energy flows vary due to a slight change in input temperature T_M via thermal sensitivity parameters. We notice that η^L_{TM} and η^R_{TM} remain nearly constant within the region $0.05T \leqslant T_M \leqslant 0.15T$. As $\eta^M_{TM} \approx 0$, we establish the input terminal resistance to be very large. We then define the following parameters for the transistor operating region $0.05T \leqslant T_M \leqslant 0.15T$:

(i) thermal conductance

$$c = \frac{J_L}{T_M - T_R}, \tag{39}$$

(ii) output thermal resistance

$$r_e = \frac{T_L - T_R}{J_L}, \tag{40}$$

and we visualize the variation of c (Fig. 10) with the control bath temperature T_M. Here, we keep T_L and T_R fixed. We now vary T_L to understand the variation of r_e by keeping T_M and T_R constant as in (Fig. 11). The variation of c, with respect to T_M, shows a behavior similar to the variation of transconductance with the gate voltage of an electronic field effect transistor (FET). As the temperature of the hot bath T_L increases, thermal resistance r_e decreases. This can be further reduced by keeping T_L fixed but increasing T_M. The behavior of these parameters helps one to develop a small-signal model similar to FET. Hence, we express these parameters in an electronic-like circuit diagram as in Fig. 12 for more clarity.

IV. CONCLUSION

The investigations in this paper are carried out to develop a quantum thermal transistor model using the quantum trajectory method, drawing inspiration from its electronic counterpart. Our previous work analyzed thermal transistor models to investigate average dynamics and energy flows. We further extended our research to examine the environmental effects of these models. This paper explored the stochastic behavior resulting from continuous monitoring in the baths. By performing weak measurements, we derived a stochastic master equation. Then, we solved it using the Euler-Maryuma approximation to find a numerical solution and get the appropriate quantum trajectories for the transistor model. Even though this technique is commonly used in classical systems, we approximated it to be used in a quantum system. We demonstrated the possibility of establishing a small-signal model with appropriate tuning for weak measurements. We then identified thermal conductance and output thermal resistance parameters for our thermal transistor small-signal model. We also visualized how continuous monitoring can introduce fluctuations in the average energy flow. This type of analysis helps us understand the impact of noise during conditioning. In future work, we will be investigating how to incorporate feedback control into this system. Our model's limitations stem from selecting the particular measurement scheme and the approximations used. Here, we considered a diffusion trajectory based on a modified measurement strategy inspired by the homodyne measurement technique.

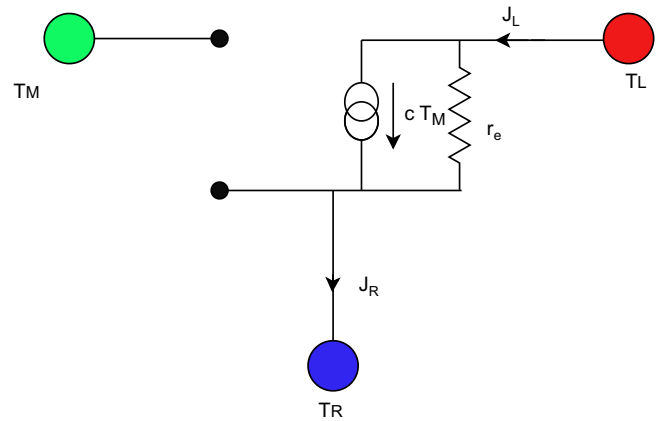

FIG. 12. The diagram expresses the parameters c and r_e. This is the small-signal equivalent of the quantum thermal transistor.

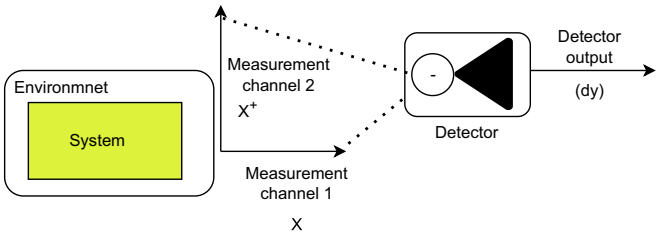

FIG. 13. The visualization of the detection process.

Consequently, the dynamics and energy flows revolve around this selected quantum trajectory. Nevertheless, the main goal of this paper is to establish a platform for constructing thermal analogous models to electronic components while giving prominence to their possible nonlinear/stochastic behavior, due to the disturbances in the surrounding environment. Thus, we hope our findings will contribute to realizing a more practical design of a quantum thermal transistor.

ACKNOWLEDGMENTS

U.N.E. would like to thank R.T. Wijesekara for his support and insightful discussions on thermal transistor models and members of AχL at Monash University for their constant encouragement and support. The work of U.N.E is supported by Monash Graduate Scholarship (MGS).

APPENDIX A: TWO-LEVEL SYSTEM

We adopt the simplest system [54] for our analysis, which is the two-level system whose energy levels are placed $\hbar\omega$ apart, with $\hbar$ representing the reduced Planck constant. The Hamiltonian for this system has the form

$$\hat{H} = \frac{\hbar\omega}{2}\hat{\sigma}_z, \tag{A1}$$

where $\hat{\sigma}_z$ is the Pauli matrix in the z direction. We define the raising and lowering operators for the system that interacts with the thermal baths as

$$\hat{\sigma}^- = \begin{pmatrix} 0 & 1 \\ 0 & 0 \end{pmatrix},$$
$$\hat{\sigma}^+ = \begin{pmatrix} 0 & 0 \\ 1 & 0 \end{pmatrix}. \tag{A2}$$

We assume that the baths' interactions are along in the x direction, hence the selection of these as our system operators to describe the quantum trajectory in Eq. (1). The Hamiltonian for the TLS-bath interaction can then be described as

$$\hat{H}_{\text{TLS-bath}} = \sum_k \hbar(\hat{\sigma}^- g_k \hat{b}_k + \hat{\sigma}^+ g_k \hat{b}_k^\dagger). \tag{A3}$$

with g_k as the coupling constant between TLS and the corresponding bath operator, and $\hat{b}_k$, and $\hat{b}_k^\dagger$ as bath annihilation and creation operators.

APPENDIX B: DERIVING THE STOCHASTIC MASTER EQUATION FROM STOCHASTIC SCHRÖDINGER EQUATION

As we study a continuously fluctuating signal like an energy flow and having nonzero temperature thermal baths, the most intuitive way is to approximate that as a diffusive stochastic equation. At strictly positive temperatures, only pure diffusion-type equations remain [39]. In comparison to the most general nonlinear stochastic Schrödinger equation (SSE) for a diffusive case, it is possible to build an Ito-type stochastic differential equation to a TLS as in Refs. [13,14,33,34,52,69–73]:

$$\begin{aligned} \mathrm{d}|\psi\rangle = \Big[& \mathrm{d}W_1(t)\sqrt{\gamma_\uparrow}(\hat{\sigma}^- - \langle\hat{\sigma}^-\rangle) + \mathrm{d}W_2(t)\sqrt{\gamma_\downarrow}(\hat{\sigma}^+ - \langle\hat{\sigma}^+\rangle) - \frac{i}{\hbar}\hat{H}\mathrm{d}t \\ & - \frac{\mathrm{d}t}{2}\gamma_\uparrow(\hat{\sigma}^+\hat{\sigma}^- - 2\langle\hat{\sigma}^+\rangle\hat{\sigma}^- + \langle\hat{\sigma}^+\rangle\langle\hat{\sigma}^-\rangle) - \frac{\mathrm{d}t}{2}\gamma_\downarrow(\hat{\sigma}^-\hat{\sigma}^+ - 2\langle\hat{\sigma}^-\rangle\hat{\sigma}^+ + \langle\hat{\sigma}^-\rangle\langle\hat{\sigma}^+\rangle)\Big]|\psi\rangle, \end{aligned} \tag{B1}$$

where the dissipation rates are represented as $\gamma_\uparrow = \mathcal{J}(\omega)[1 + N(\omega)]$ and $\gamma_\downarrow = \mathcal{J}(\omega)N(\omega)$. Here, $\mathcal{J}(\omega)$ corresponds to the spectral density function of the thermal bath, and $N(\omega)$ corresponds to the population of harmonic oscillator mode with frequency ω in a thermal bath with temperature T approximated by the Planck distribution $N(\omega) = \{\exp(\frac{\hbar\omega}{k_B T}) - 1\}^{-1}$. Also, $\langle\hat{\sigma}^+\rangle = \langle\psi|\hat{\sigma}^+|\psi\rangle$ and $\langle\hat{\sigma}^-\rangle = \langle\psi|\hat{\sigma}^-|\psi\rangle$. Moreover, $\mathrm{d}W_1(t)$ and $\mathrm{d}W_2(t)$ satisfy $\mathrm{d}W_1(t)\mathrm{d}W_2(t) = \delta_{12}dt$, with δ representing the Kronecker delta. This shows the input noise from uncorrelated channels. For an ensemble, we can represent the evolution of states [52] as

$$\mathrm{d}\overline{\rho}(t) = |\mathrm{d}\psi(t)\rangle\langle\psi(t)| + |\psi(t)\rangle\langle\mathrm{d}\psi(t)| + |\mathrm{d}\psi(t)\rangle\langle\mathrm{d}\psi(t)|. \tag{B2}$$

Next, we use the following Ito rules:

$$\begin{aligned} (\mathrm{d}t)^2 &= 0, \\ [\mathrm{d}W_{1,2}(t)]\mathrm{d}t &= 0, \\ [\mathrm{d}W_{1,2}(t)]^2 &= 0, \end{aligned} \tag{B3}$$

and expand Eq. (B2) using Eq. (B1) as

$$\begin{aligned}
\mathrm{d}\overline{\rho}(t) = &\Big[\mathrm{d}W_1(t)\sqrt{\gamma_\uparrow}(\hat{\sigma}^- - \langle\hat{\sigma}^-\rangle) + \mathrm{d}W_2(t)\sqrt{\gamma_\downarrow}(\hat{\sigma}^+ - \langle\hat{\sigma}^+\rangle) - \frac{i}{\hbar}\hat{H}\mathrm{d}t - \frac{\mathrm{d}t}{2}\gamma_\uparrow(\hat{\sigma}^+\hat{\sigma}^- - 2\langle\hat{\sigma}^+\rangle\hat{\sigma}^- + \langle\hat{\sigma}^+\rangle\langle\hat{\sigma}^-\rangle)\\
&- \frac{\mathrm{d}t}{2}\gamma_\downarrow(\hat{\sigma}^-\sigma_j^+ - 2\langle\hat{\sigma}^-\rangle\hat{\sigma}^+ + \langle\hat{\sigma}^-\rangle\langle\hat{\sigma}^+\rangle)\Big]\overline{\rho}(t)\\
&+ \overline{\rho}(t)\Big[\mathrm{d}W_1(t)\sqrt{\gamma_\uparrow}(\hat{\sigma}^+ - \langle\hat{\sigma}^+\rangle) + \mathrm{d}W_2(t)\sqrt{\gamma_\downarrow}(\hat{\sigma}^- - \langle\hat{\sigma}^-\rangle) + \frac{i}{\hbar}\hat{H}\mathrm{d}t - \frac{\mathrm{d}t}{2}\gamma_\uparrow(\hat{\sigma}^-\hat{\sigma}^+ - 2\langle\hat{\sigma}^-\rangle\hat{\sigma}^+ + \langle\hat{\sigma}^-\rangle\langle\hat{\sigma}^+\rangle)\\
&- \frac{\mathrm{d}t}{2}\gamma_\downarrow(\hat{\sigma}^+\sigma_j^- - 2\langle\hat{\sigma}^+\rangle\hat{\sigma}^- + \langle\hat{\sigma}^+\rangle\langle\hat{\sigma}^-\rangle)\Big]\\
&+ \mathrm{d}t\gamma_\uparrow[\hat{\sigma}^-\overline{\rho}(t)\hat{\sigma}^+ - \langle\hat{\sigma}^+\rangle\hat{\sigma}^-\overline{\rho}(t) - \overline{\rho}(t)\langle\hat{\sigma}^-\rangle\hat{\sigma}^+ + \langle\hat{\sigma}^-\rangle\langle\hat{\sigma}^+\rangle\overline{\rho}(t)]\\
&+ \mathrm{d}t\gamma_\downarrow[\hat{\sigma}^+\overline{\rho}(t)\hat{\sigma}^- - \langle\hat{\sigma}^+\rangle\hat{\sigma}^-\overline{\rho}(t) - \overline{\rho}(t)\langle\hat{\sigma}^-\rangle\hat{\sigma}^+ + \langle\hat{\sigma}^-\rangle\langle\hat{\sigma}^+\rangle\overline{\rho}(t)]. \qquad \text{(B4)}
\end{aligned}$$

Simplifying, we arrive at the stochastic master equation (SME):

$$\begin{aligned}
\mathrm{d}\overline{\rho}(t) = &-\frac{i}{\hbar}[\hat{H}, \overline{\rho}(t)]\mathrm{d}t + \mathcal{L}[\overline{\rho}(t)]\mathrm{d}t + \sqrt{\gamma_\uparrow}[\hat{\sigma}^-\overline{\rho}(t) + \overline{\rho}(t)\hat{\sigma}^+ - (\langle\hat{\sigma}^-\rangle\overline{\rho}(t) + \overline{\rho}(t)\langle\hat{\sigma}^+\rangle)]\mathrm{d}W_1(t)\\
&+ \sqrt{\gamma_\downarrow}[\hat{\sigma}^+\overline{\rho}(t) + \overline{\rho}(t)\hat{\sigma}^- - (\langle\hat{\sigma}^+\rangle\overline{\rho}(t) + \overline{\rho}(t)\langle\hat{\sigma}^-\rangle)]\mathrm{d}W_2(t), \qquad \text{(B5)}
\end{aligned}$$

where

$$\mathcal{L}[\overline{\rho}(t)] = \gamma_\uparrow\big(\hat{\sigma}^-\overline{\rho}(t)\hat{\sigma}^+ - \tfrac{1}{2}\{\hat{\sigma}^+\hat{\sigma}^-, \overline{\rho}(t)\}\big) + \gamma_\downarrow\big(\hat{\sigma}^+\overline{\rho}(t)\hat{\sigma}^- - \tfrac{1}{2}\{\hat{\sigma}^-\hat{\sigma}^+, \overline{\rho}(t)\}\big). \qquad \text{(B6)}$$

Here, the two measurement channels can occur simultaneously, with independent Wiener noise for the two channels. As per discussions in Refs. [14,52], we approximate the two measurement strengths of the two channels, k_1 and k_2, to a single measurement channel, similar to that of a homodyne measurement process. A simple schematic of this measurement is given in Fig. 13. This removes the independence of the Wiener noise for the two channels, invoking some correlation between them. Thus, we represent with a single noise source, representing the conditioned evolution as

$$\begin{aligned}
\mathrm{d}\rho(t) = &-\frac{i}{\hbar}[\hat{H}, \rho(t)]\mathrm{d}t + \mathcal{L}[\rho(t)]\mathrm{d}t + \Bigg[\sqrt{\frac{k_1}{k_1+k_2}\gamma_\uparrow}\{\sigma^-\rho(t) + \rho(t)\sigma^+ - [\langle\sigma^-\rangle\rho(t) + \rho(t)\langle\sigma^+\rangle]\}\\
&- \sqrt{\frac{k_2}{k_1+k_2}\gamma_\downarrow}\{\sigma^+\rho(t) + \rho(t)\sigma^- - [\langle\sigma^+\rangle\rho(t) + \rho(t)\langle\sigma^-\rangle]\}\Bigg]\mathrm{d}W(t). \qquad \text{(B7)}
\end{aligned}$$

Note that this type of an inefficient and approximated measurement now changes the overall knowledge of the system. Hence, we introduce a new quantum state ρ for the system. Then, we represent Eq. (B7) as

$$\begin{aligned}
\mathrm{d}\rho(t) = &-\frac{i}{\hbar}[\hat{H}, \rho(t)]\mathrm{d}t + \mathcal{L}[\rho(t)]\mathrm{d}t + \sqrt{\eta_1\gamma_\uparrow}\{\hat{\sigma}^-\rho(t) + \rho(t)\hat{\sigma}^+ - [\langle\hat{\sigma}^-\rangle\rho(t) + \rho(t)\langle\hat{\sigma}^+\rangle]\}\mathrm{d}W(t)\\
&- \sqrt{\eta_2\gamma_\downarrow}\{\hat{\sigma}^+\rho(t) + \rho(t)\hat{\sigma}^- - [\langle\hat{\sigma}^+\rangle\rho(t) + \rho(t)\langle\hat{\sigma}^-\rangle]\}\mathrm{d}W(t), \qquad \text{(B8)}
\end{aligned}$$

We define a threshold for the measurement strengths to approximate a quantum trajectory in a thermal state inspired by the works in [51]. We consider the measurement strengths as $k_1 = \mathcal{J}(\omega)[1 + N(\omega)]$ and $k_2 = \mathcal{J}(\omega)N(\omega)$, where ω represents the angular frequency between the two levels [51,52]. Thus,

$$\begin{aligned}
\eta_{1,T} &= \frac{1 + N(\omega)}{1 + 2N(\omega)},\\
\eta_{2,T} &= \frac{N(\omega)}{1 + 2N(\omega)} \qquad \text{(B9)}
\end{aligned}$$

Hence, we rearrange Eq. (B8), introducing an efficiency parameter $\zeta[0, 1]$, as

$$\begin{aligned}
\mathrm{d}\rho_r(t) = &-\frac{i}{\hbar}[\hat{H}, \rho(t)]\mathrm{d}t + \mathcal{L}[\rho(t)]\mathrm{d}t + \sqrt{\frac{\mathcal{J}(\omega)\zeta}{1 + 2N(\omega)}}[1 + N(\omega)]\{\hat{\sigma}^-\rho(t) + \rho(t)\hat{\sigma}^+ - [\langle\hat{\sigma}^-\rangle\rho(t) + \rho(t)\langle\hat{\sigma}^+\rangle]\}\mathrm{d}W(t)\\
&+ \sqrt{\frac{\mathcal{J}(\omega)\zeta}{1 + 2N(\omega)}}[-N(\omega)]\{\hat{\sigma}^+\rho(t) + \rho(t)\hat{\sigma}^- - [\langle\hat{\sigma}^+\rangle\rho(t) + \rho(t)\langle\hat{\sigma}^-\rangle]\}\mathrm{d}W(t). \qquad \text{(B10)}
\end{aligned}$$

We introduce ζ to keep the measurement strength as weak as possible so that continuous monitoring does not affect the overall transistor dynamics. Now, let us extend Eq. (B5) to incorporate three TLSs that are strongly coupled. We need to derive the

stochastic master equation, which describes the evolution of a system with three strong TLSs coupled in contact with a heat bath undergoing indirect measurements [39]. We take the interaction to link the energy of the TLS P to the position of each harmonic oscillator that comprises the bath as

$$\hat{H}^{\mathrm{P}}_{\text{sys-bath}} = \hbar\hat{\sigma}^{x}_{\mathrm{P}} \sum_{k} g^{\mathrm{P}}_{k}\left(\hat{b}^{\mathrm{P}}_{k} + \hat{b}^{\mathrm{P}\dagger}_{k}\right). \tag{B11}$$

Here, $\hat{\sigma}^{x}_{P}$, are expanded Pauli matrices such that

$$\begin{aligned}\hat{\sigma}^{x}_{L} &= \hat{\sigma}^{x} \otimes \hat{I} \otimes \hat{I},\\ \hat{\sigma}^{x}_{M} &= \hat{I} \otimes \hat{\sigma}^{x} \otimes \hat{I},\\ \hat{\sigma}^{x}_{R} &= \hat{I} \otimes \hat{I} \otimes \hat{\sigma}^{x}.\end{aligned} \tag{B12}$$

Then, we define the system jump operators as

$$\hat{A}_{\mathrm{P}}(\omega) = \sum_{\epsilon'-\epsilon=\hbar\omega} |\epsilon\rangle\langle\epsilon|\sigma^{x}_{\mathrm{P}}|\epsilon'\rangle\langle\epsilon'| = \hat{\sigma}^{-}_{\mathrm{P}}, \tag{B13}$$

$$\hat{A}^{\dagger}_{\mathrm{P}}(\omega) = \sum_{\epsilon'-\epsilon=-\hbar\omega} |\epsilon\rangle\langle\epsilon|\sigma^{x}_{\mathrm{P}}|\epsilon'\rangle\langle\epsilon'| = \hat{\sigma}^{+}_{\mathrm{P}}, \tag{B14}$$

defined for $\mathrm{P} \in \{L, M, R\}$, considering the system Hamiltonian $\hat{H}_{\text{sys}} = \sum_i \epsilon_i|\epsilon_i\rangle\langle\epsilon_i|$. This replaces the operators $\sqrt{\gamma_\uparrow}\sigma^{-}$ and $\sqrt{\gamma_\downarrow}\sigma^{+}$ in Eq. (B5) as $\sqrt{\mathcal{J}_{\mathrm{P}}(\omega)[1+N_{\mathrm{P}}(\omega)]}\hat{A}_{\mathrm{P}}(\omega)$ and $\sqrt{\mathcal{J}_{\mathrm{P}}(\omega)N_{\mathrm{P}}(\omega)}\hat{A}^{\dagger}_{\mathrm{P}}(\omega)$ respectively to suit the complex system of three TLSs. Now, ω represents all the possible energy transitions that can happen in the system. Here, we consider the spectral density of the baths as,

$$\mathcal{J}_{\mathrm{P}}(\omega) = \sum_{k} 2\pi \left|g^{\mathrm{P}}_{k}\right|^{2} \delta(\omega - \omega_k), \tag{B15}$$

with $|g^{\mathrm{P}}_{k}|$ representing the coupling strength between kth bath mode ω_k and TLS P. We select a system Hamiltonian that is already digonalizable in the bare states. Hence, the first term vanishes as there is no Hamiltonian evolution. This results in the master equation

$$\begin{aligned}\mathrm{d}\overline{\rho}(t) = &\sum_{P\in(L,M,R)} \mathcal{L}_{\mathrm{P}}[\overline{\rho}(t)]\mathrm{d}t + \sum_{\omega>0}\sqrt{\mathcal{J}_{L}(\omega)[1+N_{\mathrm{L}}(\omega)]}[\hat{A}_{L}(\omega)\overline{\rho}(t) + \overline{\rho}(t)\hat{A}^{\dagger}_{L}(\omega) - [\langle\hat{A}_{L}(\omega)\rangle\overline{\rho}(t) + \overline{\rho}(t)\langle\hat{A}^{\dagger}_{L}(\omega)\rangle]]\mathrm{d}W_1(t)\\
&+ \sum_{\omega>0}\sqrt{\mathcal{J}_{L}(\omega)N_{\mathrm{L}}(\omega)}[\hat{A}^{\dagger}_{L}(\omega)\overline{\rho}(t) + \overline{\rho}(t)\hat{A}_{L}(\omega) - [\langle\hat{A}^{\dagger}_{L}(\omega)(t)\rangle\overline{\rho} + \overline{\rho}(t)\langle\hat{A}_{L}(\omega)\rangle]]\mathrm{d}W_2(t)\\
&+ \sum_{\omega>0}\sqrt{\mathcal{J}_{M}(\omega)[1+N_{\mathrm{M}}(\omega)]}[\hat{A}_{M}(\omega)\overline{\rho}(t) + \overline{\rho}(t)\hat{A}^{\dagger}_{M}(\omega) - [\langle\hat{A}_{M}(\omega)\rangle\overline{\rho}(t) + \overline{\rho}(t)\langle\hat{A}^{\dagger}_{M}(\omega)\rangle]]\mathrm{d}W_3(t)\\
&+ \sum_{\omega>0}\sqrt{\mathcal{J}_{M}(\omega)N_{\mathrm{M}}(\omega)}[\hat{A}^{\dagger}_{M}(\omega)\overline{\rho}(t) + \overline{\rho}(t)\hat{A}_{M}(\omega) - [\langle\hat{A}^{\dagger}_{M}(\omega)\rangle\overline{\rho}(t) + \overline{\rho}(t)\langle\hat{A}_{M}(\omega)\rangle]]\mathrm{d}W_4(t)\\
&+ \sum_{\omega>0}\sqrt{\mathcal{J}_{R}(\omega)[1+N_{\mathrm{R}}(\omega)]}[\hat{A}_{R}(\omega)\overline{\rho}(t) + \overline{\rho}(t)\hat{A}^{\dagger}_{R}(\omega) - [\langle\hat{A}_{R}(\omega)\rangle\overline{\rho}(t) + \overline{\rho}(t)\langle\hat{A}^{\dagger}_{R}(\omega)\rangle]]\mathrm{d}W_5(t)\\
&+ \sum_{\omega>0}\sqrt{\mathcal{J}_{R}(\omega)N_{\mathrm{R}}(\omega)}[\hat{A}^{\dagger}_{R}(\omega)\overline{\rho}(t) + \overline{\rho}(t)\hat{A}_{R}(\omega) - [\langle\hat{A}^{\dagger}_{R}(\omega)\rangle\overline{\rho}(t) + \overline{\rho}(t)\langle\hat{A}_{R}(\omega)\rangle]]\mathrm{d}W_6(t),\end{aligned} \tag{B16}$$

where

$$\begin{aligned}\mathcal{L}_{\mathrm{P}}[\overline{\rho}(t)] = \sum_{\omega>0}\Bigg[&\mathcal{J}_{\mathrm{P}}(\omega)[1+N_{\mathrm{P}}(\omega)]\left(\hat{A}_{\mathrm{P}}(\omega)\overline{\rho}(t)\hat{A}^{\dagger}_{\mathrm{P}}(\omega) - \frac{1}{2}\{\hat{A}^{\dagger}_{\mathrm{P}}(\omega)\hat{A}_{\mathrm{P}}(\omega), \overline{\rho}(t)\}\right) + \mathcal{J}_{\mathrm{P}}(\omega)N_{\mathrm{P}}(\omega)\\
&\times\left(\hat{A}^{\dagger}_{\mathrm{P}}(\omega)\overline{\rho}(t)\hat{A}_{\mathrm{P}}(\omega) - \frac{1}{2}\{\hat{A}_{\mathrm{P}}(\omega)\hat{A}^{\dagger}_{\mathrm{P}}(\omega), \overline{\rho}(t)\}\right)\Bigg].\end{aligned} \tag{B17}$$

Reference [51] describes a similar continuous measurement of the environment as the optimal strategy. Here, we have six measurement channels, happening simultaneously. In order to quantify weak measurements, and for computational simplicity, we obtain an approximate measurement as per the discussions above for a single TLS-bath inefficient measurement trajectory.

Hence, we modify Eq. (B16) to

$$\begin{aligned} \mathrm{d}\rho(t) = & \sum_{\mathrm{P}\in(L,M,R)} \mathcal{L}_{\mathrm{P}}[\rho(t)]\mathrm{d}t + \sum_{\mathrm{P}\in(L,M,R)} \sum_{\omega>0} \sqrt{\eta_{\mathrm{P},1}\mathcal{J}_{\mathrm{P}}(\omega)[1+N_{\mathrm{P}}(\omega)]}(\hat{A}_{\mathrm{P}}(\omega)\rho(t) + \rho(t)\hat{A}^{\dagger}_{\mathrm{P}}(\omega) \\ & - [\langle \hat{A}_{\mathrm{P}}(\omega)\rangle \rho(t) + \rho(t)\langle \hat{A}^{\dagger}_{\mathrm{P}}(\omega)\rangle])\mathrm{d}W_{\mathrm{P}}(t) - \sum_{\mathrm{P}\in(L,M,R)} \sum_{\omega>0} \sqrt{\eta_{\mathrm{P},2}\mathcal{J}_{\mathrm{P}}(\omega)N_{\mathrm{P}}(\omega)}(\hat{A}^{\dagger}_{\mathrm{P}}(\omega)\rho(t) + \rho(t)\hat{A}_{\mathrm{P}}(\omega) \\ & - [\langle \hat{A}^{\dagger}_{\mathrm{P}}(\omega)\rangle \rho(t) + \rho(t)\langle \hat{A}_{\mathrm{P}}(\omega)\rangle])\mathrm{d}W_{\mathrm{P}}(t). \end{aligned} \tag{B18}$$

Further, introducing measurement thresholds and control parameter ζ, we represent Eq. (B18) as

$$\begin{aligned} \mathrm{d}\rho(t) = & \sum_{\mathrm{P}\in(L,M,R)} \mathcal{L}_{\mathrm{P}}[\rho(t)]\mathrm{d}t + \sum_{\mathrm{P}\in(L,M,R)} \sum_{\omega>0} \sqrt{\frac{\mathcal{J}_{\mathrm{P}}(\omega)\zeta}{1+2N_{\mathrm{P}}(\omega)}}[1+N_{\mathrm{P}}(\omega)](A_{\mathrm{P}}(\omega)\rho(t) + \rho(t)\hat{A}^{\dagger}_{\mathrm{P}}(\omega) \\ & - [\langle A_{\mathrm{P}}(\omega)\rangle \rho(t) + \rho(t)\langle \hat{A}^{\dagger}_{\mathrm{P}}(\omega)\rangle])\mathrm{d}W_{\mathrm{P}}(t) + \sum_{\mathrm{P}\in(L,M,R)} \sum_{\omega>0} \sqrt{\frac{\mathcal{J}_{\mathrm{P}}(\omega)\zeta}{1+2N_{\mathrm{P}}(\omega)}}[-N_{\mathrm{P}}(\omega)](\hat{A}^{\dagger}_{\mathrm{P}}(\omega)\rho(t) + \rho(t)\hat{A}_{\mathrm{P}}(\omega) \\ & - [\langle \hat{A}^{\dagger}_{\mathrm{P}}(\omega)\rangle \rho(t) + \rho(t)\langle A_{\mathrm{P}}(\omega)\rangle])\,\mathrm{d}W_{\mathrm{P}}(t)\,, \end{aligned} \tag{B19}$$

where $\langle \hat{A}_{\mathrm{P}}(\omega)\rangle = \mathrm{Tr}[\rho(t)\hat{A}_{\mathrm{P}}(\omega)]$ and $\langle \hat{A}^{\dagger}_{\mathrm{P}}(\omega)\rangle = \mathrm{Tr}[\rho(t)\hat{A}^{\dagger}_{\mathrm{P}}(\omega)]$.

[1] T. Werlang, M. A. Marchiori, M. F. Cornelio, and D. Valente, Optimal rectification in the ultrastrong coupling regime, Phys. Rev. E **89**, 062109 (2014).

[2] K. Joulain, J. Drevillon, Y. Ezzahri, and J. Ordonez-Miranda, Quantum thermal transistor, Phys. Rev. Lett. **116**, 200601 (2016).

[3] B.-Q. Guo, T. Liu, and C.-S. Yu, Multifunctional quantum thermal device utilizing three qubits, Phys. Rev. E **99**, 032112 (2019).

[4] M. Majland, K. S. Christensen, and N. T. Zinner, Quantum thermal transistor in superconducting circuits, Phys. Rev. B **101**, 184510 (2020).

[5] R. T. Wijesekara, S. D. Gunapala, M. I. Stockman, and M. Premaratne, Optically controlled quantum thermal gate, Phys. Rev. B **101**, 245402 (2020).

[6] A. Mandarino, K. Joulain, M. D. Gómez, and B. Bellomo, Thermal transistor effect in quantum systems, Phys. Rev. Appl. **16**, 034026 (2021).

[7] R. T. Wijesekara, S. D. Gunapala, and M. Premaratne, Darlington pair of quantum thermal transistors, Phys. Rev. B **104**, 045405 (2021).

[8] A. Mandarino, Quantum thermal amplifiers with engineered dissipation, Entropy **24**, 1031 (2022).

[9] N. Gupt, S. Bhattacharyya, B. Das, S. Datta, V. Mukherjee, and A. Ghosh, Floquet quantum thermal transistor, Phys. Rev. E **106**, 024110 (2022).

[10] R. T. Wijesekara, S. D. Gunapala, and M. Premaratne, Towards quantum thermal multitransistor systems: Energy divider formalism, Phys. Rev. B **105**, 235412 (2022).

[11] Y.-Q. Liu, D.-H. Yu, and C.-S. Yu, Common environmental effects on quantum thermal transistor, Entropy **24**, 32 (2021).

[12] U. N. Ekanayake, S. D. Gunapala, and M. Premaratne, Engineered common environmental effects on multitransistor systems, Phys. Rev. B **107**, 075440 (2023).

[13] H. Wiseman and L. Diósi, Complete parameterization, and invariance, of diffusive quantum trajectories for markovian open systems, J. Chem. Phys. **268**, 91 (2001).

[14] K. Jacobs and D. A. Steck, A straightforward introduction to continuous quantum measurement, Contemp. Phys. **47**, 279 (2006).

[15] K. Sekimoto, *Stochastic Energetics* (Springer, Berlin, 2010).

[16] J. M. Horowitz, Quantum-trajectory approach to the stochastic thermodynamics of a forced harmonic oscillator, Phys. Rev. E **85**, 031110 (2012).

[17] F. W. J. Hekking and J. P. Pekola, Quantum jump approach for work and dissipation in a two-level system, Phys. Rev. Lett. **111**, 093602 (2013).

[18] G. P. Martins, N. K. Bernardes, and M. F. Santos, Continuous monitoring of energy in quantum open systems, Phys. Rev. A **99**, 032124 (2019).

[19] H. Zhao and L. Nie, Brownian thermal control device, Eur. Phys. J. B **93** (2020).

[20] A. Devi, S. D. Gunapala, M. I. Stockman, and M. Premaratne, Nonequilibrium cavity qed model accounting for dipole-dipole interaction in strong-, ultrastrong-, and deep-strong-coupling regimes, Phys. Rev. A **102**, 013701 (2020).

[21] K. Herath and M. Premaratne, Generalized model for the charge transport properties of dressed quantum hall systems, Phys. Rev. B **105**, 035430 (2022).

[22] K. Herath and M. Premaratne, Floquet engineering of dressed surface plasmon polariton modes in plasmonic waveguides, Phys. Rev. B **106**, 235422 (2022).

[23] K. Herath, S. D. Gunapala, and M. Premaratne, A floquet engineering approach to optimize Schottky junction-based surface plasmonic waveguides, Sci. Rep. **13**, 10692 (2023).

[24] W. Zhu, I. D. Rukhlenko, and M. Premaratne, Light amplification in zero-index metamaterial with gain inserts, Appl. Phys. Lett. **101**, 031907 (2012).

[25] H. Hapuarachchi, S. Mallawaarachchi, H. T. Hattori, W. Zhu, and M. Premaratne, Optoelectronic figure of merit of a metal nanoparticle—quantum dot (MNP-QD) hybrid molecule for assessing its suitability for sensing applications, J. Phys.: Condens. Matter **30**, 054006 (2018).

[26] I. B. Udagedara, I. D. Rukhlenko, and M. Premaratne, Complex-ω approach versus complex-k approach in description of gain-assisted surface plasmon-polariton propagation along linear chains of metallic nanospheres, Phys. Rev. B **83**, 115451 (2011).

[27] S. Mallawaarachchi, M. Premaratne, S. D. Gunapala, and P. K. Maini, Tuneable superradiant thermal emitter assembly, Phys. Rev. B **95**, 155443 (2017).

[28] C. Jayasekara, M. Premaratne, S. D. Gunapala, and M. I. Stockman, MoS_2 spaser, J. Appl. Phys. **119**, 133101 (2016).

[29] H.-P. Breuer and F. Petruccione, *The Theory of Open Quantum Systems* (Oxford University Press, Oxford, 2007), pp. 109–218.

[30] H. M. Wiseman and G. J. Milburn, Interpretation of quantum jump and diffusion processes illustrated on the Bloch sphere, Phys. Rev. A **47**, 1652 (1993).

[31] A. T. Barun, A simple model of quantum trajectories, Am. J. Phys **70** (2002).

[32] R. Carballeira, D. Dolgitzer, P. Zhao, D. Zeng, and Y. Chen, Stochastic Schrödinger equation derivation of non-Markovian two-time correlation functions, Sci. Rep. **11**, 11828 (2021).

[33] M. Campisi, J. Pekola, and R. Fazio, Nonequilibrium fluctuations in quantum heat engines: theory, example, and possible solid state experiments, New J. Phys. **17**, 035012 (2015).

[34] G. Manzano and R. Zambrini, Quantum thermodynamics under continuous monitoring: A general framework, AVS Quantum Sci. **4**, 025302 (2022).

[35] B. Bhandari and A. N. Jordan, Continuous measurement boosted adiabatic quantum thermal machines, Phys. Rev. Res. **4**, 033103 (2022).

[36] J. Lu, R. Wang, C. Wang, and J.-H. Jiang, Brownian thermal transistors and refrigerators in mesoscopic systems, Phys. Rev. B **102**, 125405 (2020).

[37] C. Elouard, N. K. Bernardes, A. R. R. Carvalho, M. F. Santos, and A. Auffèves, Probing quantum fluctuation theorems in engineered reservoirs, New J. Phys. **19**, 103011 (2017).

[38] F. Salari Sehdaran, M. Bina, C. Benedetti, and M. G. A. Paris, Quantum probes for Ohmic environments at thermal equilibrium, Entropy **21**, 486 (2019).

[39] S. Attal and C. Pellegrini, Stochastic master equations in thermal environment, Open Syst. Inf. Dyn. **17**, 389 (2010).

[40] C. Pellegrini, Markov chains approximation of jump-diffusion stochastic master equations, Ann. Inst. H. Poincaré (B) Probab. Stat. **46**, 924 (2010).

[41] S. Mandt, D. Sadri, A. A. Houck, and H. E. Türeci, Stochastic differential equations for quantum dynamics of spin-boson networks, New J. Phys. **17**, 053018 (2015).

[42] M. G. Genoni, S. Mancini, H. M. Wiseman, and A. Serafini, Quantum filtering of a thermal master equation with a purified reservoir, Phys. Rev. A **90**, 063826 (2014).

[43] C. Pellegrini and F. Petruccione, Diffusion approximation of stochastic master equations with jumps, J. Math. Phys. **50**, 122101 (2009).

[44] M. Bayram, T. Partal, and G. Orucova Buyukoz, Numerical methods for simulation of stochastic differential equations, Adv. Differ. Equ. **2018**, 17 (2018).

[45] W. Verstraelen and M. Wouters, Gaussian quantum trajectories for the variational simulation of open quantum-optical systems, Appl. Sci. **8**, 1427 (2018).

[46] P. Warszawski, H. M. Wiseman, and A. C. Doherty, Solving quantum trajectories for systems with linear Heisenberg-picture dynamics and Gaussian measurement noise, Phys. Rev. A **102**, 042210 (2020).

[47] P. Rouchon, A tutorial introduction to quantum stochastic master equations based on the qubit/photon system, Annu. Rev. Control **54**, 252 (2022).

[48] P. Meystre and M. Sargent, *Elements of Quantum Optics* (Springer, Berlin, 2013).

[49] J. F. Ralph, S. Maskell, M. Ransom, and H. Ulbricht, Classical tracking for quantum trajectories, in *Proceedings of the 24th International Conference on Information Fusion* (IEEE, Piscataway, 2021).

[50] G. Casati and C. Mejía-Monasterio, Classical and quantum chaos and control of heat flow, J. Korean Phys. Soc. (2007).

[51] M. G. Genoni, S. Mancini, and A. Serafini, Optimal feedback control of linear quantum systems in the presence of thermal noise, Phys. Rev. A **87**, 042333 (2013).

[52] H. Wiseman and G. Milburn, *Quantum Measurement and Control* (Cambridge University Press, Cambridge, 2010).

[53] A. Caldeira and A. Leggett, Quantum tunnelling in a dissipative system, Ann. Phys. (NY) **149**, 374 (1983).

[54] H. A. R. T. Wijesekara, Quantum thermo-optical devices, Ph.D. thesis, Monash University, 2022.

[55] Stochastic Taylor expansion, Lecture Notes, https://math.nyu.edu/~cai/Courses/Derivatives/compfin_lecture_5.pdf.

[56] A. Chia and H. M. Wiseman, Quantum theory of multiple-input–multiple-output Markovian feedback with diffusive measurements, Phys. Rev. A **84**, 012120 (2011).

[57] J. E. Gough, M. R. James, H. I. Nurdin, and J. Combes, Quantum filtering for systems driven by fields in single-photon states or superposition of coherent states, Phys. Rev. A **86**, 043819 (2012).

[58] M. Crescimanno, Quantum-mechanics and thermal noise in dissipative systems, Ann. Phys. (NY) **223**, 229 (1993).

[59] M. Premaratne and G. P. Agrawal, *Theoretical Foundations of Nanoscale Quantum Devices* (Cambridge University Press, Cambridge, 2021).

[60] D. Reiche, J.-T. Hsiang, and B.-L. Hu, Quantum thermodynamic uncertainty relations, generalized current fluctuations and nonequilibrium fluctuation-dissipation inequalities, Entropy **24**, 1016 (2022).

[61] K. Jacobs, *Quantum Measurement Theory and its Applications* (Cambridge University Press, Cambridge, 2014).

[62] A. A. Clerk, M. H. Devoret, S. M. Girvin, F. Marquardt, and R. J. Schoelkopf, Introduction to quantum noise, measurement, and amplification, Rev. Mod. Phys. **82**, 1155 (2010).

[63] A. Barchielli and B. Vacchini, Quantum Langevin equations for optomechanical systems, New J. Phys. **17**, 083004 (2015).

[64] A. Agarwal and J. Lang, *Foundations of Analog and Digital Electronic Circuits* (Elsevier Science, Amsterdam, 2005).

[65] See Supplemental Material at http://link.aps.org/supplemental/10.1103/PhysRevB.108.235421 for quantum thermal transistor stochastic model code.

[66] R. Sánchez, B. Sothmann, and A. N. Jordan, Heat diode and engine based on quantum Hall edge states, New J. Phys. **17**, 075006 (2015).

[67] R. Sánchez, B. Sothmann, and A. N. Jordan, Effect of incoherent scattering on three-terminal quantum Hall thermoelectrics, Phys. E **75**, 86 (2016).

[68] J. Yang, C. Elouard, J. Splettstoesser, B. Sothmann, R. Sánchez, and A. N. Jordan, Thermal transistor and thermometer based on Coulomb-coupled conductors, Phys. Rev. B **100**, 045418 (2019).

[69] C. W. Gardiner and M. J. Collett, Input and output in damped quantum systems: Quantum stochastic differential equations and the master equation, Phys. Rev. A **31**, 3761 (1985).

[70] A. Barchielli and M. Gregoratti, *Quantum Trajectories and Measurements in Continuous Time: The Diffusive Case*, Lecture Notes in Physics Vol. 782 (Springer, Berlin, 2009).

[71] C. Viviescas, I. Guevara, A. R. R. Carvalho, M. Busse, and A. Buchleitner, Entanglement dynamics in open two-qubit systems via diffusive quantum trajectories, Phys. Rev. Lett. **105**, 210502 (2010).

[72] D. Farina, V. Cavina, M. G. Genoni, and V. Giovannetti, Entanglement-assisted, noise-assisted, and monitoring-enhanced quantum bath tagging, Phys. Rev. A **106**, 042609 (2022).

[73] B. Bhandari, R. Czupryniak, P. A. Erdman, and A. N. Jordan, Measurement-based quantum thermal machines with feedback control, Entropy **25**, 204 (2023).